Soils and Foundations 2015;55(1):201–212

HOSTED BY

The Japanese Geotechnical Society

Soils and Foundations

www.sciencedirect.com
journal homepage: www.elsevier.com/locate/sandf

Measurements of driving energy in SPT and various dynamic cone penetration tests

Tatsunori Matsumoto[a,*], Le Ta Phan[b], Akihiko Oshima[c], Shinya Shimono[a]

[a]*Kanazawa University, Kanazawa, Japan*
[b]*Ho Chi Minh City University of Architecture, Ho Chi Minh City, Viet Nam*
[c]*Osaka City University, Osaka, Japan*

Received 14 April 2014; received in revised form 22 September 2014; accepted 21 October 2014
Available online 2 January 2015

Abstract

Driving energy was measured in a standard penetration test (SPT) and 12 types of dynamic cone penetration tests (DCPTs) having different configurations for the hammer, driving rod, anvil and cone tip. The driving energy transferred from the free falling hammer to the driving rod was estimated from the measurements of strain and acceleration below the anvil. Basically, the driving energy was estimated for 21 successive blows in order to obtain the mean value, the standard deviation (σ) and the coefficient of variance (COV) in the SPT and DCPTs. The dynamic cone resistance, q_{dyn}, was estimated from the driving energy, the corresponding set per blow, and masses of the hammer and the total rods. Thus, the estimated dynamic cone resistance was compared with the static cone resistance, q_t, from a cone penetration test (CPT). The main objective of this report is to provide information on the driving efficiency in the SPT and each DCPT. The mean values for e_f in the tests ranged from 52% to 76%. The values of COV for e_f ranged from 0.024 to 0.265. Even though the test results are limited, the dynamic cone resistance, q_t, estimated from the dynamic measurements were relatively good measures of the cone resistance from the CPT, showing the importance of the dynamic measurement in the SPT and DCPTs.

In addition, possible factors influencing the driving efficiency, such as the hammer mass, the configuration of the driving rod (solid or hollow), the ratio of the diameter of the anvil and the diameter of the hammer, and the existence of a cushion or cushions between the anvil and the hammer, are discussed on the basis of the limited test results.

Keywords: Driving energy; Driving efficiency; Dynamic cone penetration test; Standard penetration test; Dynamic measurements; Cone resistance; IGC:C03; C07

1. Introduction

After the 2011 off the Pacific Coast of Tohoku Earthquake, the Research Committee on Prediction of Damages of Housing Sites due to Liquefaction based on Low-cost and High Reliable Site Investigation Methods (hereafter called the research committee) was formed in the Japanese Geotechnical Society in 2012, with the aim of investigating the potential of various site investigation methods, such as CPTs, Swedish sounding (SWS), dynamic cone penetration tests, simple soil sampling and so on, to estimate the potential liquefaction of soils quickly and cost-effectively. In the course of the activities of the research committee, comparative SPT, CPT, DCPT and SWS tests were carried out at a site in Shiga Prefecture, Japan. Dynamic cone penetration tests, DCPTs, may be regarded as complementary to the SPT, since soil sampling does not accompany DCPTs.

*Corresponding author.
E-mail address: matsumoto@se.kanazawa-u.ac.jp (T. Matsumoto).
Peer review under responsibility of The Japanese Geotechnical Society.

http://dx.doi.org/10.1016/j.sandf.2014.12.016

In order to correlate the blow count, N_d, from the various types of DCPTs with the SPT blow count, N, or the driving resistance, the driving energy actually transmitted to the driving rod is useful information. Measurements of the driving energy in the SPT have been carried out in many researches (e.g., Kovacs, 1979; Schmertmann, 1979; Schmertmann and Alejandro, 1979; Kovacs and Salomone, 1982; Yokel, 1982; Skempton, 1986; Matsumoto et al., 1992; Robertson et al., 1992; Morgano and Liang, 1992; Abou-maatar et al., 1996; Robertson and Wride, 1997; Fujita and Ohno, 2000; Ishihara et al., 2004; Rodrigues et al., 2008; Cavalcante et al., 2008). In contrast, measurements of the driving energy in dynamic cone penetration tests have been limited, except for Michi et al. (2004) and Žaržojus et al. (2013).

Fig. 1. Location of the test site.

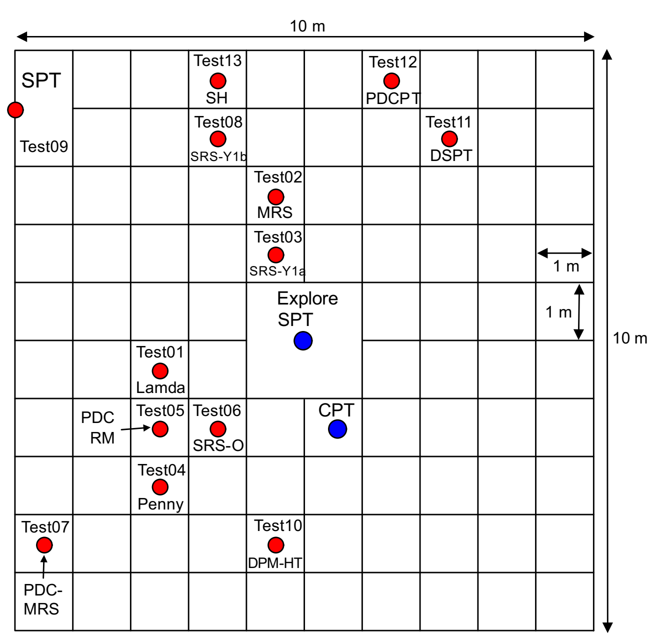

Fig. 2. Locations of explore SPT and CPT, and measurements of driving energy in SPT and DCPTs.

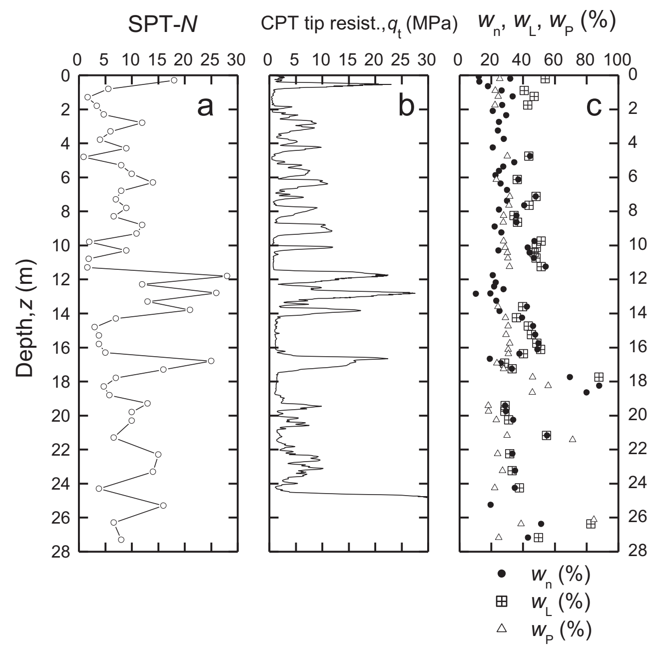

Fig. 3. Typical results from the explore SPT.

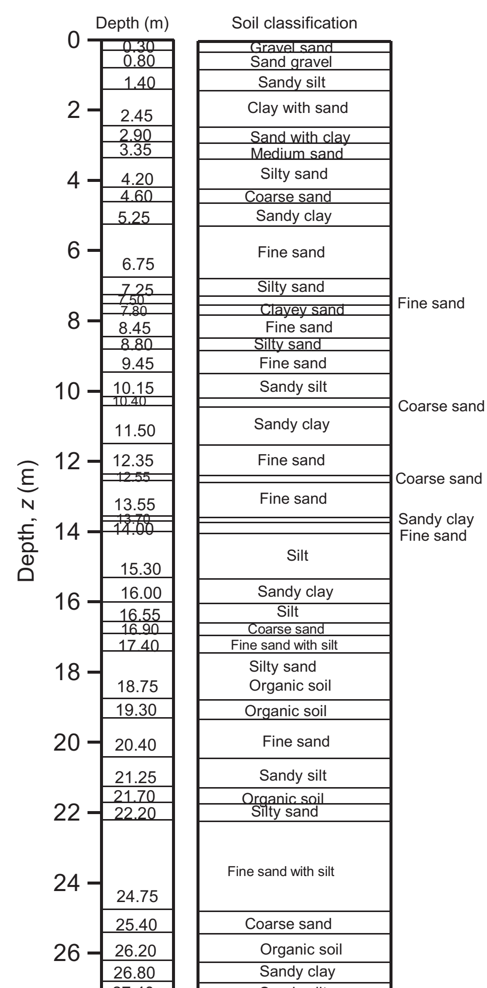

Fig. 4. Soil profile at the location of explore SPT.

Hence, the driving energy was measured for the standard penetration test (SPT) and 12 types of DCPTs having different configurations for the hammer, driving rod, anvil and cone tip. Basically, the driving energy was estimated for 21 successive blows in order to obtain the mean value, the standard deviation (σ) and the coefficient of variance (COV) in the SPT and DCPTs. The dynamic cone resistance was estimated from the driving energy and the corresponding set per blow. Thus, the estimated dynamic cone resistance could be compared with the static cone resistance from the cone penetration test (CPT). The main objective of this report is to provide information on the driving efficiency in the SPT and various DCPT configurations. In addition, possible factors influencing the driving efficiency, such as the hammer mass, the configuration of the driving rod (solid or hollow), the ratio of the diameter of the anvil and the diameter of the hammer, the existence of a cushion or cushions between the anvil and the hammer, are discussed.

2. Outline of the site

The test site was located in Shiga Prefecture, close to Biwa Lake, the largest lake in Japan (Fig. 1). The test area, 10 m × 10 m, was divided into 100 grids, as shown in Fig. 2. Various site investigations, such as SPT, CPT, DCPT, SWS and soil sampling, were carried out in each grid. Note that the locations for the SPT and DCPTs, with dynamic measurements, are indicated in Fig. 2, together with the locations of the explore SPT and CPT.

The groundwater table at the test site was 0.74 m below the ground level. The distributions with the depth of the SPT blow count, N, the tip resistance, q_t, from the CPT, the natural water content, w_n, the liquid limit, w_L and the plastic limit, w_P, that were obtained from the disturbed soil samples from the SPT are shown in Fig. 3. The soil profile at the test site, derived from the SPT, is shown in Fig. 4, based on the Japan Unified Soil Classification System (JGS 0051, 2009) that is equivalent to ISO 14688-2 (2004). It is seen from these figures that the test ground is categorised as a sandy ground and that the ground is relatively uniform to a depth of 10 m.

The tests were carried in only two days in November 2012, by a total of 12 testing companies and institutes. The tests were carried out in parallel. As a set of dynamic measurement system was available, it was difficult to measure the dynamic signals of all the blows in all the tests. Hence, the SPT and DCPTs with dynamic measurements were carried out in the layers of fine sand and silty sand (z=5.25 to 7.25 m). Only

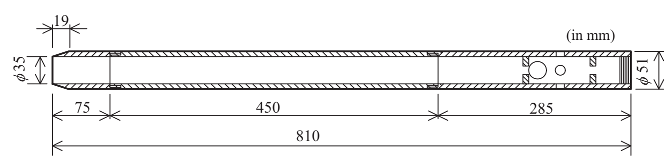

Fig. 5. Configuration of the split spoon sampler used in SPT.

Table 1
Specifications of hammer, anvil, rod, cone and nominal driving energy in SPT and DCPTs.

	Device										
	SRS-O, SRS-Y1a, SRS-Y1b	Lamda	MRS, PDC_MRS	DPM-HT	PDC_μRS	PENNY	DSPT	PDCPT	SH	SPT	
Diam. of hammer guide rod (mm)	101.6	40.5	20.0	4 0.5	15.0	30.0	19.0	16.0	16.0	40.5	
Diam. of hammer, D_h (mm)	246.0	180.0	160.0	180.0	135.0	178.0	95.0	60.0	40.0	180.0	
Diam. of anvil, D_a (mm)	175.0	97.0	90.0	75.0	35.0	51.0	50.0	50.0	40.0	71.0	
D_a/D_h	0.71	0.54	0.56	0.42	0.26	0.29	0.53	0.83	1.00	0.39	
Mass of hammer, m (kg)	63.5		30.0		20.0	30.0	10.0	5.0	3.0, 5.0	63.5	
Fall height of hammer, h (mm)	500		350		250	200	500	500		750	
Apex angle of cone (deg)	90		90		90	60	screw point	60			
Length of cone mantle (mm)	90		69		30	9	–	0		Open	Closed
Diam. of cone, D_c (mm)	45.0		36.6		25.0	35.7	33	25		O.D. 51 I. D. 35	O.D. 51
Area of cone, A_c ($\times 10^{-4}$ m^2)	15.9		10.5		4.9	10.0	8.6			10.8	20.4
Diam. of rod, D_r (mm)	32.0		28.0		19.0	20.0	19.0	16.0		40.5	
D_c/D_r	1.41		1.31		1.32	1.79	1.74	1.56		–	
Driving energy per unit area of cone, $E=mgh/A_c$ (kJ/m^2)	195.8		97.9		99.9	58.8	57.3	50.0		432.6	229.0
Category according to ISO 22476-2	DPSH (super heavy)		DPM (medium)		DPM (medium)	DPL (light)	DPL (light)	DPL (light)		–	–
Energy ratio with reference to SRS	1.0		0.50		0.51	0.30	0.29	0.26		2.21	1.17
Penetration length for counting blow numbers, L_d (m)	0.20		0.20		0.20	0.10	0.25	0.10		0.30	0.30
Correction factor for blow counts with reference to SRS, C_f	1.00		0.50		0.51	0.60	0.23	0.52		1.47	0.780

one DCPT with dynamic measurements was conducted in the layer of fine sand (z=11.35 to 12.35 m), where relatively high N-values were measured. The results for the SPT and DCPTs with dynamic signal measurements are addressed in this paper.

3. Specifications of SPT and DCPTs

Table 1 lists the specifications of the hammer, the anvil, the rod, the cone tip and the nominal driving energy in the SPT and DCPTs. Three types of SRS (Swedish Ram Sounding), called SRS-O, SRS-Y1a and SRS-Y1b, are included in the DCPTs. The configuration of the split spoon sample used in the SPT is shown in Fig. 5.

The nominal driving energy per unit area of cone, E, is defined as $E=mgh/A_c$, where A_c is the area of the cone. This value is different in the SPT and DCPTs. The penetration length, L_d, for counting the blow numbers, N_d, are also different in the SPT and DCTPs. In order to equivalently compare N_d from the different tests, a correction factor, C_f, for blow counts, with reference to SRS, is indicated in Table 1, considering the different values for E and L_d in the SPT and DCPTs:

$$C_f = \frac{E}{(E)_{SRS}} \times \frac{(L_d)_{SRS}}{L_d} \tag{1}$$

where suffix SRS means that the value is related to SRS.

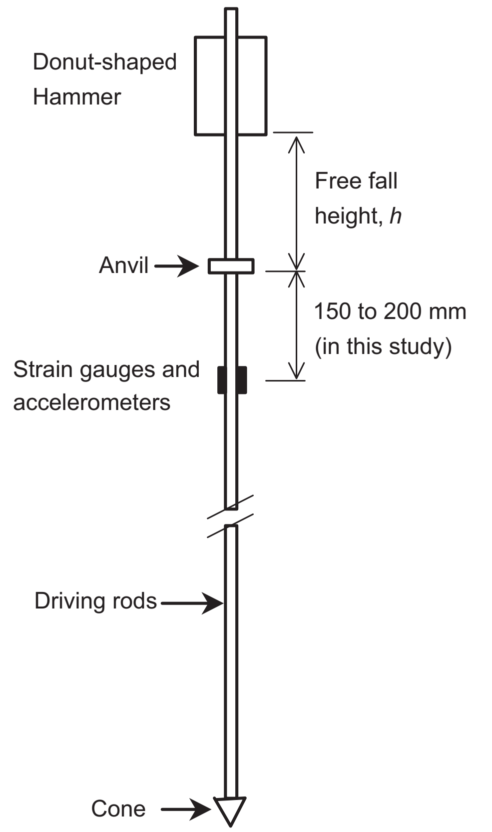

Fig. 6. Typical configuration of DCPT and dynamic measurement.

Table 2
Specification of driving rods, cushion and hammer of SPT and DCPTs, together with summary of driving energy measurements (partly duplicated with Table 1).

		Rod							**Cushion**	**Hammer**		**Ratio of dia. of anvil to hammer**	**Driving efficiency**	
Test no.	Device name	O.D. (mm)	I.D. (mm)	Area (mm^2)	Density (t/m^3)	Young's mod. (kPa)	Wave veloc. (m/s)	Total rod mass, m' (kg)		Mass, m (kg)	Fall height (mm)	D_a/D_h	Mean e_f (%)	COV of e_f
1	Lamda	32.0	–	804.2	7.647	2.06×10^8	5190	49.2	Yes	63.5	500	0.54	59.4	0.234
2	MRS	28.0	–	615.8	7.665	2.06×10^8	5184	37.8	Yes	30.0	350	0.56	74.7 (8 Blows)	0.056
3	SRS-Y1a	32.0	–	804.2	7.925	1.93×10^8	4935	51.0	Yes	63.5	500	0.71	67.5	0.059
4	Penny	20.0	–	314.2	7.671	2.00×10^8	5106	19.3	Yes	30.0	200	0.29	51.6	0.247
5	PDC (μRM)	19.0	7.0	245.0	7.590	2.06×10^8	5210	14.9	No	5.0	500	0.26	59.8	0.265
6a	SRS-O	32.0	–	804.2	7.647	2.06×10^8	5190	49.2	No	63.5	500	0.71	78.7 (16 Blows)	0.051
6b	SRS-O	32.0	–	804.2	7.647	2.06×10^8	5190	49.2	1 Sheet	63.5	500	0.71	72.7 (5 Blows)	0.024
6c	SRS-O	32.0	–	804.2	7.647	2.06×10^8	5190	49.2	2 Sheets	63.5	500	0.71	60.7 (16 Blows)	0.134
7	PDC (MRS)	28.6	18.6	370.7	8.201	2.06×10^8	5012	24.3	Yes	30.0	350	0.56	76.2	0.126
8	SRS-Y1b	32.0	16.0	603.2	7.930	1.93×10^8	4934	62.2	Yes	63.5	500	0.71	62.1	0.186
9	SPT	40.5	31.0	533.5	8.529	2.00×10^8	4843	36.4	No	63.5	750	0.39	63.0	0.090
10	DPM-HT	28.0	–	615.8	7.600	2.06×10^8	5206	37.4	Yes	30.0	350	0.42	61.2	0.058
11	DSPT	19.0	–	283.5	7.724	2.06×10^8	5164	17.5	No	10.0	500	0.53	58.1	0.113
12	PDCPT	16.0	–	201.1	7.809	2.06×10^8	5136	12.6	No	5.0	500	0.83	74.0	0.037
13a	SH	16.0	–	201.1	7.858	1.93×10^8	4956	11.1	No	3.0	500	1.0	56.1	0.037
13b	SH	16.0	–	201.1	7.858	1.93×10^8	4956	11.1	No	5.0	500	1.0	68.4	0.067

Note: O.D.=Outer diameter, I.D.=Inner diameter.
SRS=Ram Sounding MRS=Mini Ram Sounding.

As an example, if $N_d = 20$ is obtained in MRS (Mini Ram Sounding), this value corresponds to $N'_d = N_d \times C_f = 20 \times 0.5 = 10$ when compared with N_d from SRS.

Photo 1. Instrumented rods of SPT and DCPTs.

The driving energy, E_{drv}, was measured for the SPT and 12 different types of DCPTs. The specifications of the driving rods, the cushion and the hammer in the SPT and different DCPTs are listed in Table 2. Note that Test 9 is SPT and the other tests are DCPTs.

Two types of driving rods, solid and hollow cylinders, were used in the DCPTs. The values of density, ρ_r, Young's modulus, E_r, and the wave velocity, c_r, of each rod are similar, whereas the cross-sectional area, A_r, ranges widely from 200 mm^2 to 800 mm^2 due to the different configurations of the rod section.

A cushion is placed on the anvil in several tests (Tests 1–3, 6–8 and 10). In Tests 6a–c (SRS-O), the tests using no, one or two rubber membranes, each with a thickness of 2 mm, for the cushion were carried out.

The hammer mass, m, ranges widely from 3 kg to 63.5 kg. In Test 13 (SH), two types of steel hollow hammers, with masses of 3 kg (Test 13a) and 5 kg (Test 13b), are used

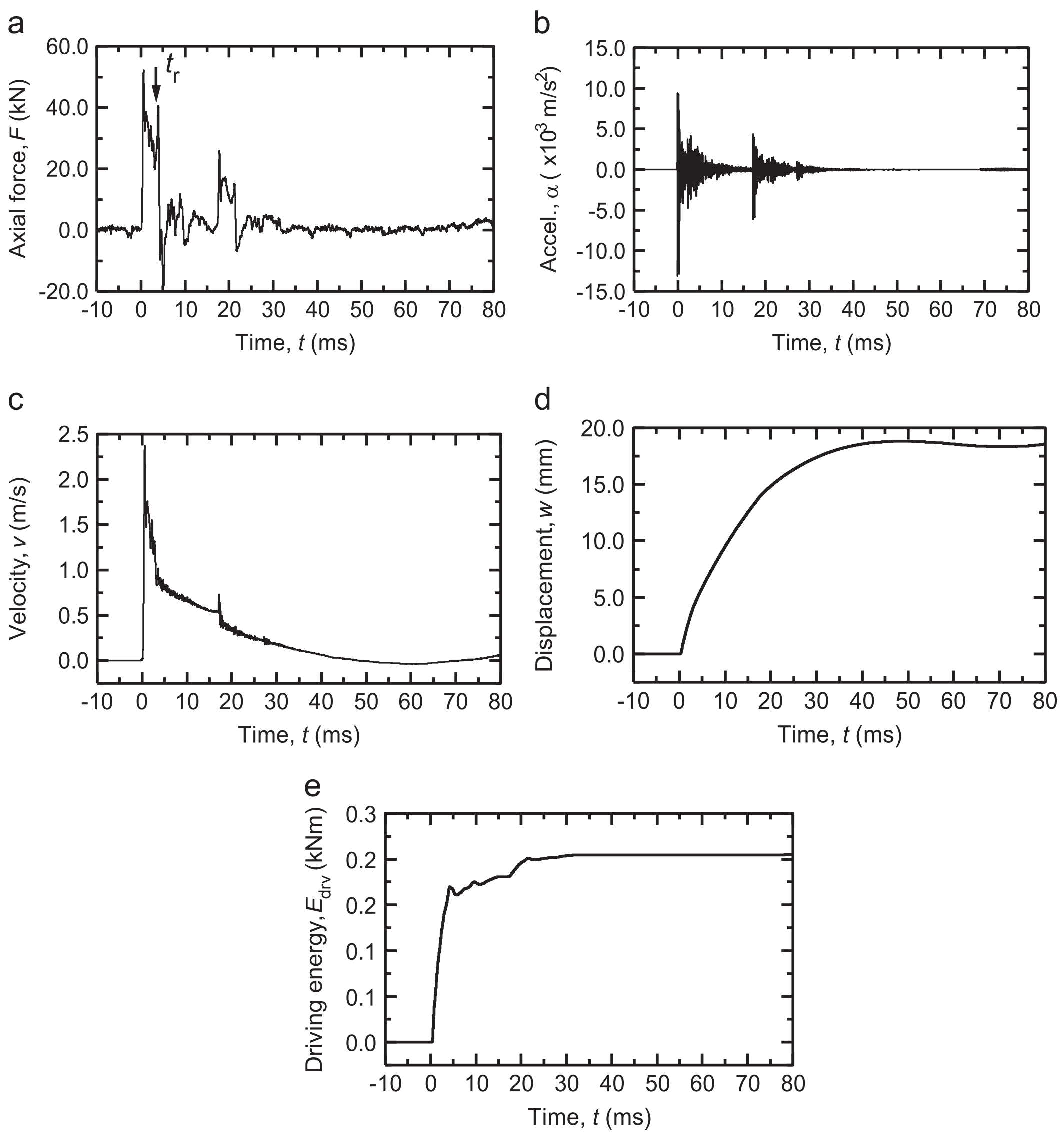

Fig. 7. Example of measured dynamic signals in SPT and results of analysis. (a) Measured force in the driving rod, (b) measured acceleration in the driving rod, (c) calculated velocity, (d) calculated displacement and (e) calculated driving energy.

according to penetration resistance, i.e., the lighter and heavier hammers are used for the lower and higher penetration resistances, respectively. Tests 13a and 13b were undertaken to investigate the influence of the hammer mass on the driving efficiency in the same DCPT device.

The difference between SPT and DCPTs is the influence of the rod friction. The rod friction may be ignored in the SPT as the SPT is conducted at the bottom of a pre-bored hole, while rod friction exists in the DCPTs. In SRS and MRS, the rods are rotated 1 1/2 turns or until the maximum torque is reached at least every 1.0 m of penetration in order to measure the torque required to turn the rods and to reduce the rod friction in practice. In other DCPTs, no attempt is made to reduce the rod friction.

4. Method for measuring driving energy

The method to calculate the driving energy in the SPT and DCPTs employed in this study is similar to that employed in the previous researches.

In order to measure dynamic signals during driving, two strain gauges, with a gauge length of 2 mm, and two piezo-electric accelerometers, with a nominal capacity of 10,000 m/s^2, were mounted on the rod shaft at symmetric positions 150 to 200 mm below the base of the anvil, as shown in Fig. 6. The instrumented driving rods for the SPT and DCPTs are shown in Photo 1. The output signals from the sensors were recorded with a sampling frequency of 1000 kHz (1 μs sampling time).

The driving energy, E_{drv}, was estimated using Eq. (2) (ISO 22476-2, 2005).

$$E_{\mathrm{drv}}(t) = \int_0^t F(t) \times v(t) \times dt \tag{2}$$

where $F(t)$ and $v(t)$ are the force and the velocity of the rod at the measurement level.

$F(t)$ was calculated by Eq. (3).

$$F(t) = E_r A_r \varepsilon(t) \tag{3}$$

where E_r and A_r are Young's modulus and the cross-sectional area of the rod, respectively, and $\varepsilon(t)$ is the average of two strains measured at symmetric positions to eliminate the influence of the inevitable flexure of the driving rod during driving.

Fig. 7 shows an example of the measured dynamic signals in the SPT. The axial force rapidly increases at the instant of the impingement of the hammer (Fig. 7(a)). The force increases again at time t=3.8 m/s due to the second impingement of the

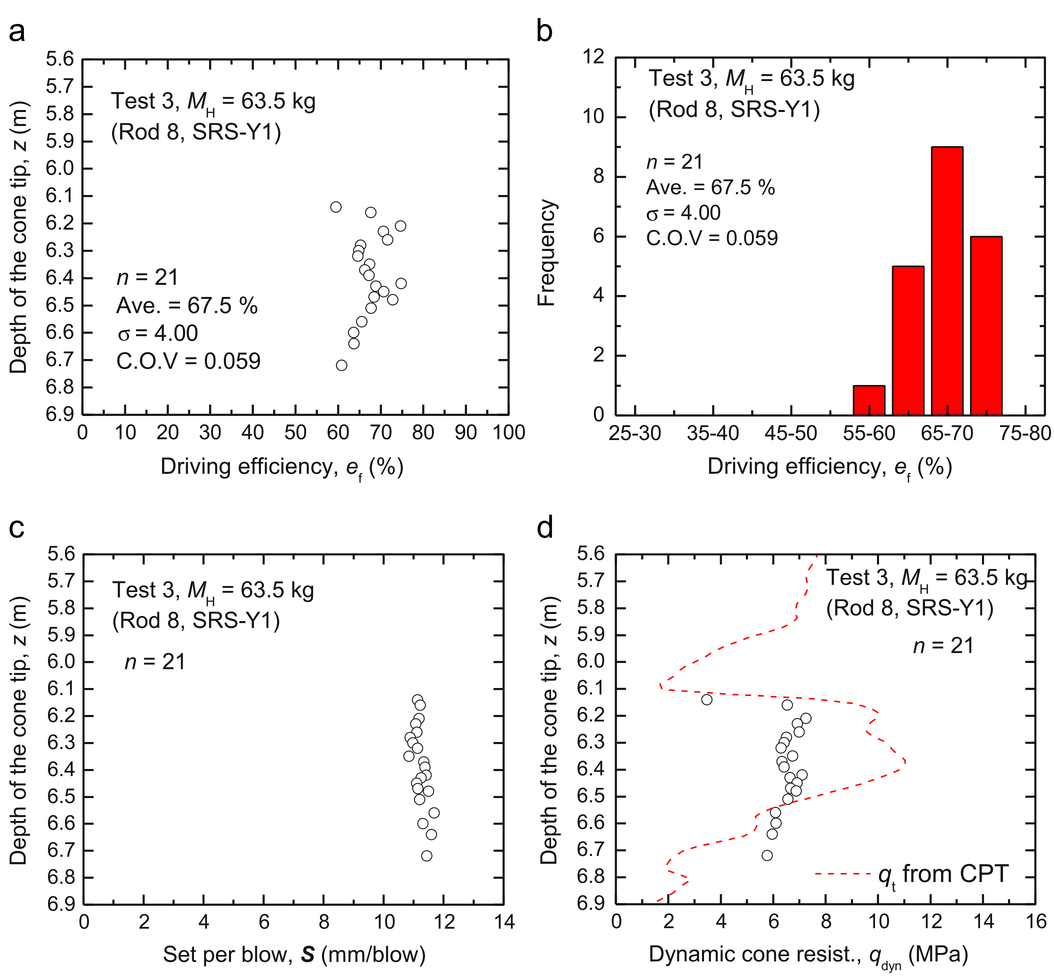

Fig. 8. Results of analyses of Test 3 (SRS-Y1a). (a) Depth vs. e_f, (b) frequency distribution of e_f, (c) depth vs. S and (d) depth vs. q_{dyn}.

hammer. As is seen from Fig. 6(b), the time evolution of the measured acceleration, α, corresponds to the above-mentioned impingements of the hammer on the anvil. However, trouble (an error) with the measurements of the accelerations was found during the data processing after the completion of the tests. The accelerometers have a nominal maximum capacity of 10,000 m/s^2. As shown in Fig. 7(b), the measured acceleration attained the maximum capacity at the first impingement of the hammer. The same trouble occurred in all the tests. Hence, to estimate the velocity, v, a special scheme was used in this study, as described in the following.

According to the one-dimensional stress-wave theory, the velocity, v, is related to the force, F, by Eq. (4) if the only downward-travelling stress-wave exists at the measuring level of the driving rod.

$$v(t) = \frac{F(t)}{\rho_r c_r A_r} \tag{4}$$

Hence, the velocity was estimated using Eq. (4) until a time, t_r, when the reflection of the incident stress-wave returned to the measuring level from the bottom level of the sampler in the case of the SPT or the cone level in the cases of the DCPTs. The time instant, t_r, can be easily determined by

$$t_r = \frac{2L_d}{c_r} \tag{5}$$

where L_d is the distance between the measuring level and the cone level.

As the downward- and upward-travelling stress-waves overlap at the measuring level after the time instant of t_r, Eq. (4) cannot be applied. Hence, the time-integration of the measured acceleration was employed after t_r.

The velocity and displacement estimated using the above-mentioned scheme are shown in Fig. 7(c) and (d), respectively. The estimated final displacement was 18 mm, which was comparable to the measured settlement per blow of 19 mm. It is seen from Fig. 7(e) that the driving energy, E_{drv}, transferred to the driving rod from the hammer increases rapidly just after the first impingement of the hammer; thereafter, it gradually increases with time and finally reaches a constant value. The constant value for E_{drv} is defined as E_{meas} in this study.

The driving efficiency, e_f, is defined as

$$e_f = \frac{E_{meas}}{mgh} \tag{6}$$

The dynamic cone resistance, q_{dyn}, was estimated using Eq. (7) where the total mass, m', of the extension rods and the guiding rods is considered according to ISO 22476-2).

$$q_{dyn} = \left(\frac{m}{m+m'}\right) \times \left(\frac{E_{meas}}{A_c \times S}\right) \tag{7}$$

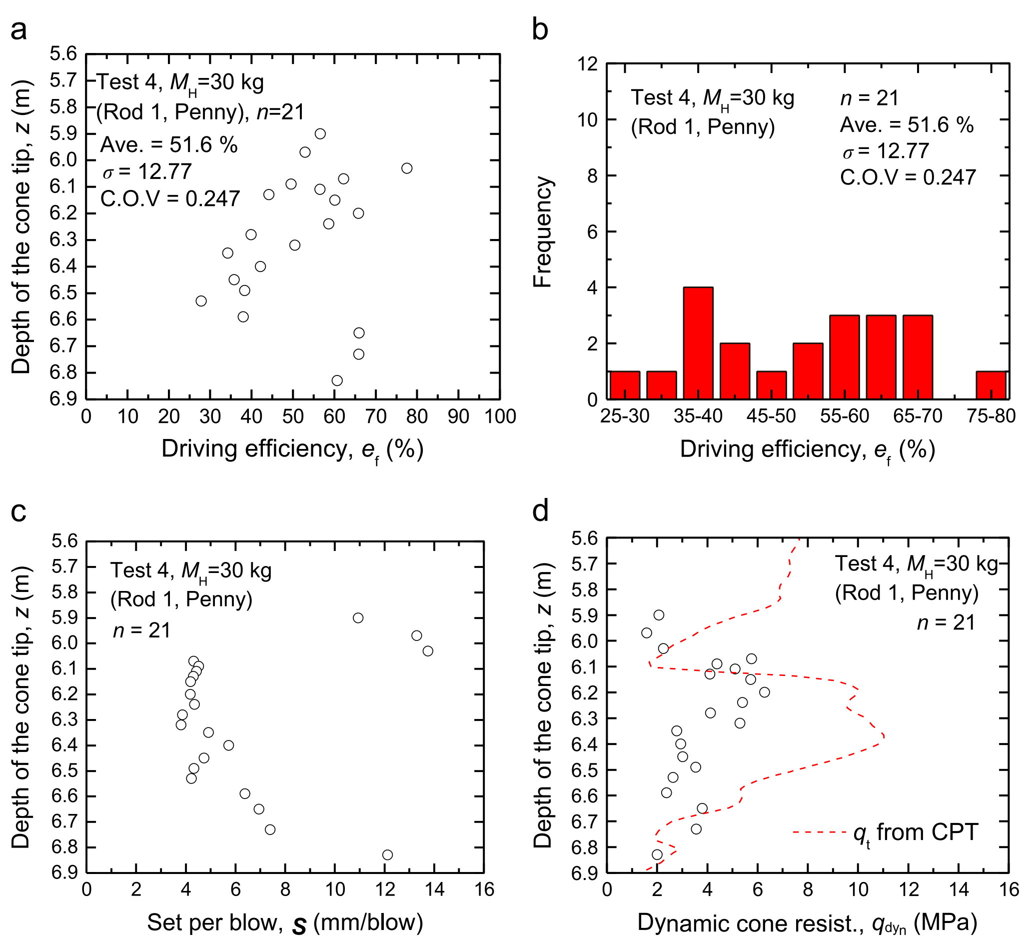

Fig. 9. Results of analyses of Test 4 (Penny). (a) Depth vs. e_f, (b) frequency distribution of e_f, (c) depth vs. S and (d) depth vs. q_{dy}.

where A_c is the cross-sectional area of the cone for each DCPT and the cross-sectional area of the sampler in the SPT assuming the fully plugging mode of the soil inside the sampler.

It should be noted that the rod friction was assumed to be 0 in Eq. (7). In other words, the influence of the rod friction, if it exists, is included in the estimated q_{dyn}. It was difficult to separate the driving resistance into the cone tip resistance and the rod friction in the tests in this study.

The above-mentioned analysis scheme was used throughout the analyses of the SPT and DCPTs with the dynamic measurements.

5. Test results

The results of Test 3 (SRS-Y1a) are shown in Fig. 8(a) depth vs. e_f; (b) frequency of e_f; (c) depth vs. S and (d) depth vs. q_{dyn} together with cone tip resistance q_t from the CPT. Test 3 was conducted at depths from 6.3 m to 6.7 m where fine sand existed (see Fig. 4). The driving efficiency, e_f, ranges from 59.8% to 72.8% with the mean values of 67.5% and COV of 0.06 having a form of a normal distribution (Fig. 8(b)). The estimated dynamic cone resistance, q_{dyn}, is of a similar order to the cone tip resistance, q_t, from the CPT. The cone tip area of the CPT was 1000 mm^2 (diameter = 35.7 mm).

The results of Test 4 (Penny) and Test 9 (SPT) are shown in Figs. 9 and 10, respectively. Test 4 had the lowest mean value and the highest value for COV of e_f among the tests in this study. The value of e_f ranges from 27.8% to 77.6% with a mean value of 51.6% and COV = 0.25. Nevertheless, the estimated dynamic cone resistance, q_{dyn}, is of a similar order and trend to the cone tip resistance, q_t, from the CPT. This result strongly indicates the advantage of DCPTs with dynamic measurements. As mentioned earlier, q_{dyn}, was estimated from E_{meas} and the measured value of S (see Eqs. (6) and (7)), not from the nominal driving energy, mgh.

The SPT is the most widely used device for sounding in Japan. A semi-automatic hammer falling device is used in Japan at present. In this particular study, however, a pulley and a rope falling method with a cathead was used for the purpose of the dynamic measurements. The mean value of e_f was 63% with COV = 0.09 (Fig. 10(a)).

It may be interesting to compare the SPT results in this study with published data. A brief comparison of the SPT results with several recent published data is made in Table 3. A detailed comparison is difficult, since the method of the falling of the hammer, the rod length below the anvil, and the test and ground conditions vary in the published data. It can be seen from Table 3 that the driving efficiency, e_f, of all the cases widely ranges from 38% to 93%, although the range in e_f for

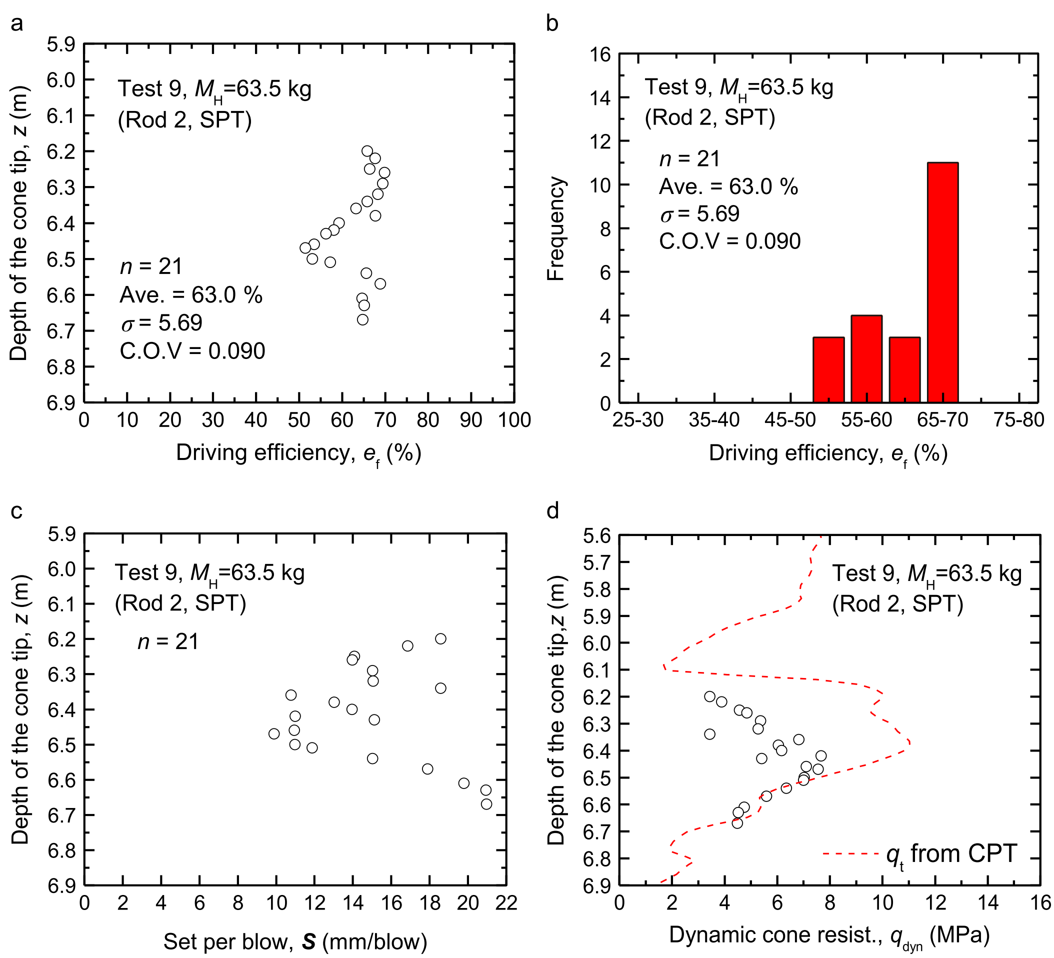

Fig. 10. Results of analyses of Test 9 (SPT). (a) Depth vs. e_f, (b) frequency distribution of e_f, (c) depth vs. S and (d) depth vs. q_{dy}.

Table 3
Brief comparison of the driving efficiencies obtained in this study and several recent publications.

Reference, country	Method of falling of hammer	Rod length below anvil (m)	Test condition, ground condition	Number of blows	Driving efficiency, e_f (%)
This study, Japan	A rope and a pulley with a cathead	8	Field Sandy soil	21	52 to 70 (average = 63%, COV = 0.09)
Matsumoto et al. (1992), Japan	A rope and a pulley without a cathead (nearly free fall)	2.5	Field Sandy soil	9	59 to 93 (average = 75%, COV = 0.18)
Fujita and Ohno (2000), Japan	A rope and a pulley without a cathead (nearly free fall)	1.8	Laboratory Model ground of dry sand	1	89
Morgano and Liang (1992), USA	Not described	3 to 30	Field Not clear	Not clear	82 to 93
Abou-maatar et al. (1996), USA	Not described	22	Field Cohesive soil and cohesionless soil	17	38 to 55
Ishihara et al. (2004), Japan	A rope and a pulley without a cathead (nearly free fall)	1.5	Laboratory Model ground of dry sand	6	79 to 91 (average = 84%, COV = 0.051)
Cavalcante et al. (2008), Brazil	Not described	2 to 10	Field Sandy clay	9	71 to 84

each case is narrower. Comparing the results in this study with three other cases in Japan, the e_f in this study is smaller than that in other cases. A possible reason is difference in hammer falling methods used in these cases. A rope and a pulley with a cathead were used in this study, while a rope and a pulley without a cathead were used in the other Japanese cases. It is thought that the friction between the rope and the cathead reduced the falling speed of the hammer in this study, resulting in lower values for e_f. A relatively large variety in the measured driving efficiencies among SPTs in Table 3 indicates the importance of measuring the actual driving energy transferred to the driving rod in order to interpret the measured N-values on the common basis.

The closed area of the Raymond sampler was used for estimating q_{dyn}. The estimated q_{dyn} values were in relatively good agreement with the cone tip resistance, q_t, in quantity and trend.

The results of the dynamic analyses for all the DCPTs are summarised in Table 2 in terms of the mean value and COV of the driving efficiency, e_f. The findings on the influential factors on e_f from the particular results are as follows:

5.1. Hammer mass

The mean estimated values, e_f, were generally around or greater than about 60% for all the tests, except for Test 4 (Penny with $m=30$ kg) and Test 13a (SH with $m=3$ kg).

In Test 13, two different hammer masses, 3 kg and 5 kg, were used in Test 13a and Test 13b, respectively. Both hammers had the same cross-section, but the heavier hammer had a larger length. The results of Test 13a and Test 13b are shown in Fig. 11. The coefficient of variance, COV, of e_f in both tests was relatively small (see Table 2). The mean e_f was greater in Test 13b where the heavier hammer mass was used. This result suggests that losses in energy, due to the imperfect impingement of the hammer and the anvil, are similar in both tests, resulting in the higher e_f for the heavier hammer (larger potential energy).

5.2. Rod type (solid rod or hollow rod)

In Test 3 (SRS-Y1a) and Test 8 (SRS-Y2b), the same test device is used, except that a solid rod is used in Test 3 while a hollow rod is used in Test 8. It should be noticed also that the length of the driving rod in Test 3 was 7 m while that was 13 m in Test 8. The frequency distributions of e_f of 21 blows in Test 3 and Test 8 are shown in Fig. 12. The mean e_f values were 67.5% (with COV=0.059) and 62.1% (with COV=0.186), respectively. In Test 8, however, two extremely small values for e_f were obtained. In order to compare the results in Test 3 and Test 8, the mean e_f and COV were calculated excluding the two values, and the mean $e_f=64.5\%$ (with COV=0.125) was obtained. Based on these results, the rod type has little influence on e_f. The rod length may also have an influence on e_f. Hence, a definite conclusion cannot be made from the measured data available in this study.

5.3. Existence of cushion

As mentioned earlier, in Test 6 (SRS-O), 2 rubber cushions having a thickness of 2 mm are used. In order to investigate the influence of the existence of a cushion/s on the driving efficiency, tests without a cushion and with one or two cushions were carried out in Tests 6a–c.

The results of Test 6 are shown in Fig. 13(a) depth vs. e_f; (b) depth vs. S, (c) depth vs. q_{dyn}. Sixteen blows were conducted for the tests with 2 cushions or no cushions, while five blows were conducted for the test with 1 cushion. The

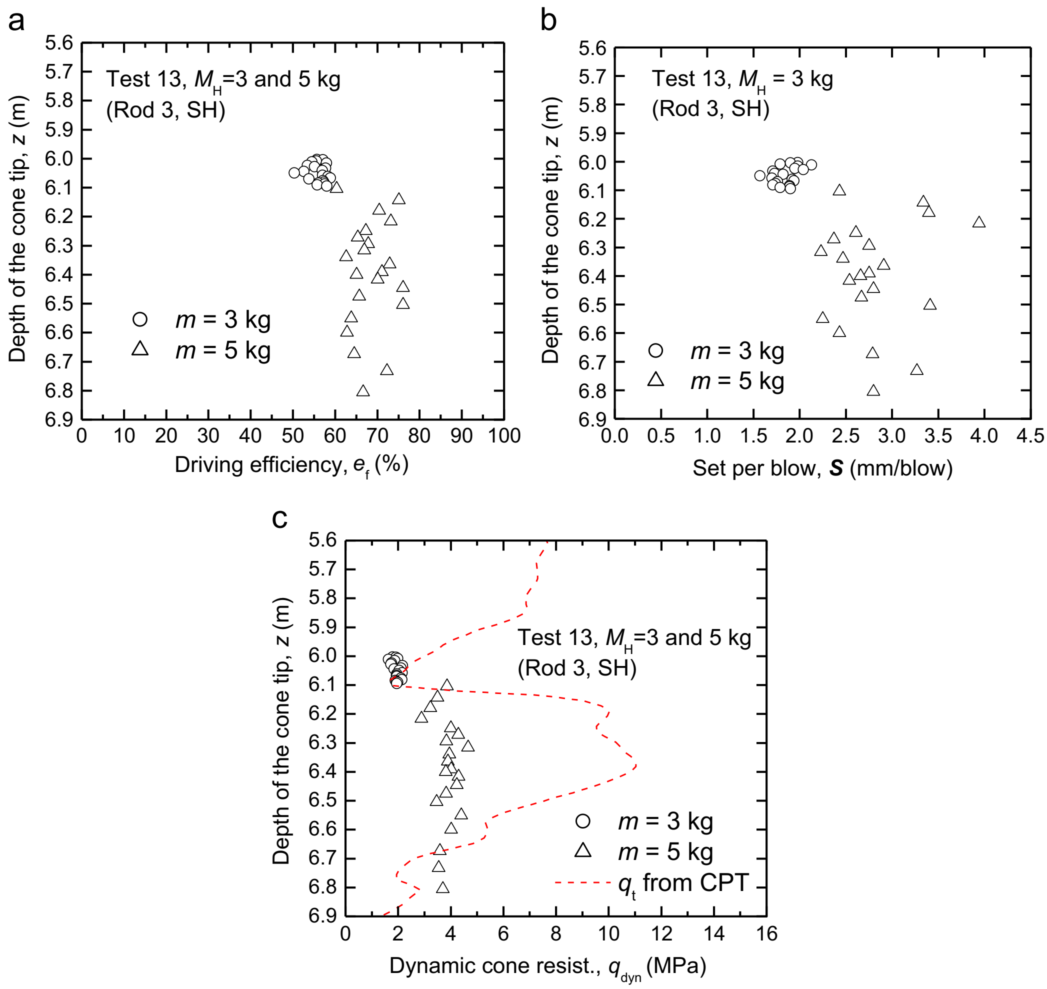

Fig. 11. Results of analyses of Test 13 (SH). (a) Depth vs. e_f, (b) depth vs. S and (c) depth vs. q_{dy}.

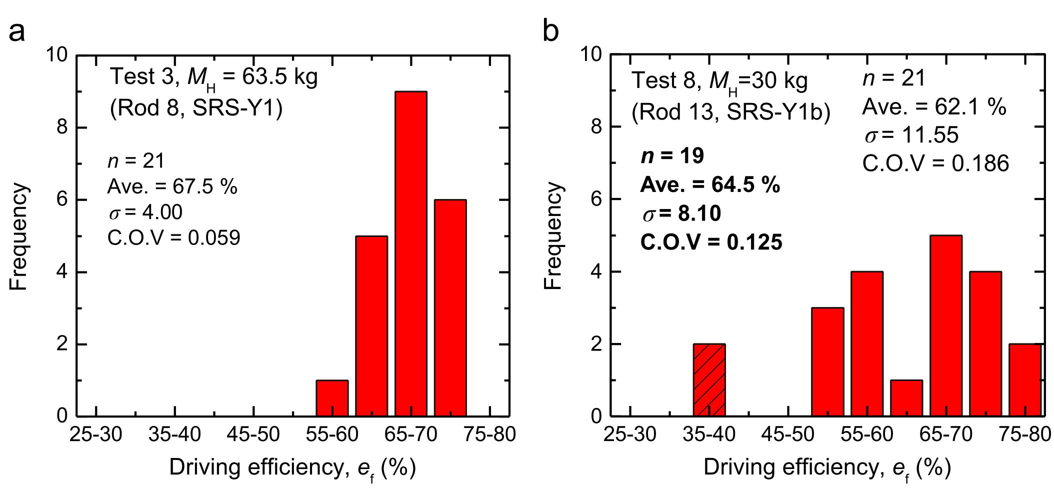

Fig. 12. Frequency distributions of e_f in Test 3 (SRS-Y1a) and Test 8 (SRS-Y1b). (a) Test 3 and (b) Test 8.

mean values for e_f were 60.7%, 72.7% and 78.7% for tests with 2, 1 and no cushions, respectively, indicating that e_f is significantly reduced when 2 cushions are used. However, in the tests with 2 cushions, the e_f values in the last 4 blows are obviously larger than those in the blows in shallower depths and are similar to the e_f values obtained in the tests with 1 or no cushion. It is seen from Fig. 13(b) that the settlements per blow, S, in the last 12 blows in the tests with 2 cushions are relatively uniform compared with the variation in e_f shown in Fig. 13(a).

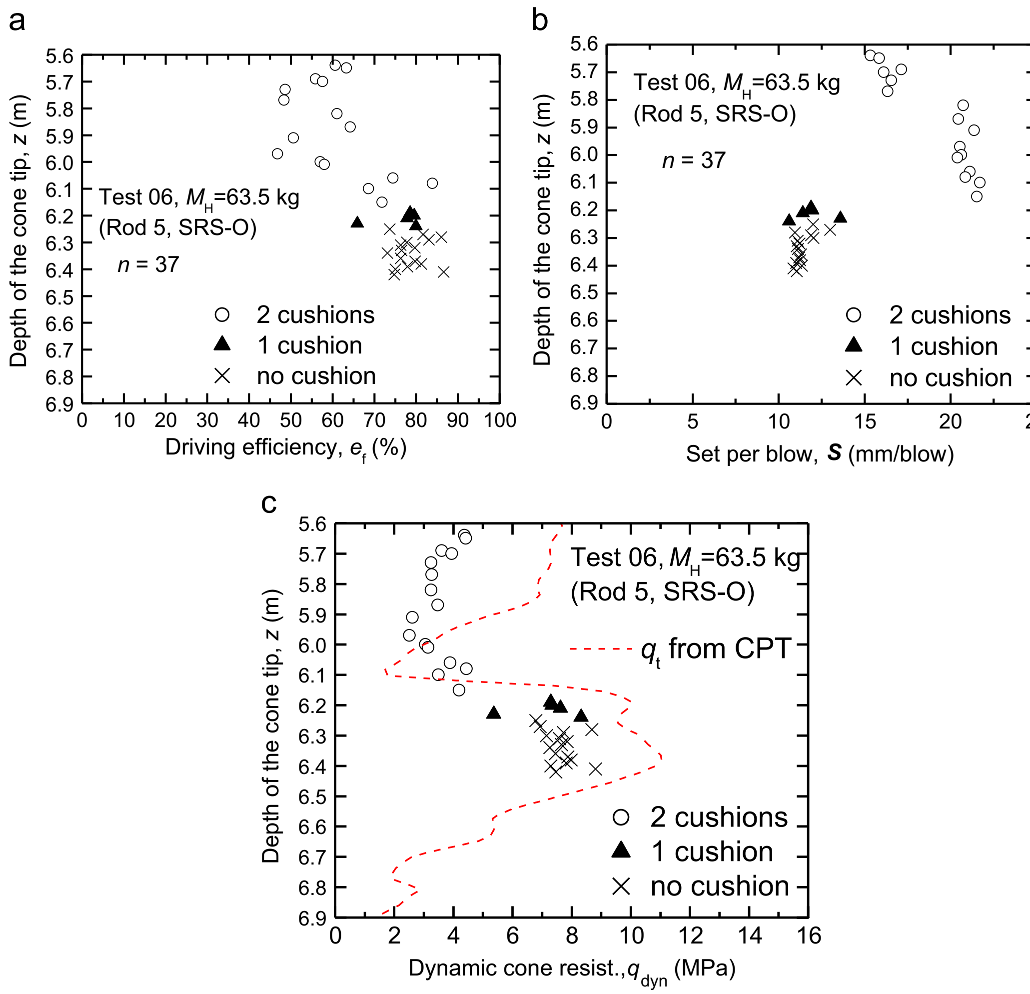

Fig. 13. Results of analyses of Test 6a, Test 6b and Test 6c. (a) Depth vs. e_f, (b) depth vs. S and (c) depth vs. q_{dyn}.

It may be noticed that the location of Test 6 was closest to the location of the CPT. It is seen from Fig. 13(c) that the profile for q_{dyn} is comparable to that for q_t from CPT regardless of the number of cushions. This result again suggests the advantage of DCPTs with dynamic measurements by which the driving energy actually transferred to the driving rod is obtained.

5.4. Ratio of anvil diameter to hammer diameter, D_a/D_h

The diameters of anvil, D_a, for Test 5 (PDC-μRS) and Test 13 (SH) are 35 mm and 40 mm, respectively. The D_a of the other tests is equal to or greater than 50 mm. The ratio of the anvil diameter to the hammer diameter, D_a/D_h, ranges from 0.26 to 1.0. In ISO 22476-2 (2005), it is prescribed that D_a shall be equal to or greater than 50 mm, and that D_a shall be equal to or less than $0.5D_h$. Based on the test results shown in Table 2, it may be said that D_a/D_h has little influence on e_f.

6. Concluding remarks

In this technical report, the driving energy actually transferred from the free falling hammer to the driving rod was measured in SPT and 12 various types of dynamic cone penetration tests (DCPTs). The mean values for the driving efficiency, e_f, in the tests ranged from 52% to 76%. The coefficients of variance, COV, of the e_f ranged from 0.024 to 0.265. The driving efficiency may be influenced by the hammer mass, the fall height of the hammer, the rod length, the penetration resistance and so on. Detailed discussions on these influences were difficult in this particular report because of the limited data and test conditions.

Even though the test results are limited, the dynamic cone resistance, q_t, estimated from the measured driving energy and set per blow (see Eqs. (6) and (7)) were relatively good measures of the cone resistance from the CPT. This indicates the importance of the dynamic measurement in SPT and DCPTs.

Acknowledgements

The authors wish to express their appreciation to the members of the Research Committee on Prediction of Damages of Residential Areas due to Liquefaction based on Low-cost and High Reliable Field Investigation Methods, formed in the Japanese Geotechnical Society from 2012 to

2014, for carrying out the dynamic cone penetration tests and SPT and for giving permission to use the measured data for this paper.

References

Abou-maatar, H., Rausche, F., Thendean, G., Likins, G., Goble, G., 1996. Wave equation soil constants from dynamic measurements on SPT. In: Proc. Fifth Int. Conf. on the Application of Stress-Wave Theory to Piles, Orlando, 163–175.

Cavalcante, E.H., Danziger, B.R., Danziger, F.B.A., 2008. On the energy reaching the sampler during SPT. In: Proc. Eighth Int. Conf. on the Application of Stress-Wave Theory to Piles, Lisbon, 737–742.

Fujita, K., Ohno, M., 2000. Stress wave theory application to standard penetration test in Japan. In: Proc. Sixth Int. Conf. on the Application of Stress-Wave Theory to Piles, São Paulo, 469–475.

Ishihara, S., Matsumoto, T., Kawano, H., 2004. Instrumented SPT in a model sand ground; driving, compression and tension tests. In: Proc. Seventh Int. Conf. on the Application of Stress-Wave Theory to Piles, Kuala Lumpur, 313–319.

ISO 14688-2, 2004. Geotechnical Investigation and Testing – Identification and Classification of Soil – Part 2: Principles for a Classification.

ISO 22476-2, 2005. Geotechnical Investigation and Testing – Field Testing – Part 2: Dynamic Probing.

JGS 0051, 2009. Method of Classification of Geomaterials for Engineering Purposes.

Kovacs, W.D., 1979. Velocity measurement of free-fall SPT hammer. J. Geotech. Eng. Div., ASCE 105 (GT1), 1–10.

Kovacs, W.D., Salomone, L.A., 1982. SPT hammer energy measurement. J. Geotech. Eng. Div., ASCE 108 (GT4), 599–620.

Matsumoto, T., Sekiguchi, H., Yoshida, H., Kita, K., 1992. Significance of two-point strain measurement in SPT. Soils Found. 32 (2), 67–82.

Michi, Y., Matsumoto, T., Ishihara, S., Shirai, N., 2004. Application of dynamic portable cone penetration tests to quality assessment of improved soil. In: Proc. Seventh Int. Conf. on the Application of Stress-Wave Theory to Piles, Kuala Lumpur, 333–340.

Morgano, C.M., Liang, R., 1992. Energy transfer in SPT—Rod length effect. In: Proc. Fourth Int. Conf. on the Application of Stress-Wave Theory to Piles, Rotterdam, 121–127.

Robertson, P.K., Woeller, D.J., Addo, K.O., 1992. Standard penetration test energy measurements using a system based on the personal computer. Can. Geotech. J. 29, 551–557.

Robertson, P.K., Wride, C.E., 1997. Cyclic liquefaction and its evaluation based on the SPT and CPT. In Proceedings of the NCEER Workshop on Evaluation of Liquefaction Resistance of Soils: Technical Report NCEER-97-0022: National Center for Earthquake Engineering Research, Buffalo, NY, pp. 41–87.

Rodrigues, C., Cavalcante, E.H., Danziger, B.R., Viana da Fonseca, A., 2008. Influence of rod type in SPT efficiency. In: Proc. Eighth Int. Conf. on the Application of Stress-Wave Theory to Piles, Lisbon, 731–736.

Schmertmann, J.H., 1979. Statics of SPT. J. Geotech. Eng. Div., ASCE 105 (GT5), 655–670.

Schmertmann, J.H., Alejandro, P., 1979. Energy dynamics of SPT. J. Geotech. Eng. Div., ASCE 105 (GT8), 909–926.

Skempton, A.W., 1986. Standard penetration test procedures and the effects in sands of overburden pressure, relative density, particle size, aging and overconsolidation: Geotechnique 36 (3), 425–447.

Yokel, F.Y., 1982. Energy transfer in standard penetration test. J. Geotech. Eng. Div., ASCE 108 (GT9), 1197–1202.

Žaržojus, G., Kelevišius, K., Amšiejus, J., 2013. Energy transfer measuring in dynamic probing test in layered geological strata. Procedia Eng. 57, 1302–1308.